HHS Public Access

Author manuscript

J Phys Chem B. Author manuscript; available in PMC 2022 May 13.

Published in final edited form as:

J Phys Chem B. 2021 May 13; 125(18): 4757–4766. doi:10.1021/acs.jpcb.1c01431.

Mechanistic Insight into the Structural Stability of Collagen Containing Biomaterials such as Bones and Cartilage

Nidhi Tiwari[a,b], **Sungsool Wi**[c], **Frederic Mentink-Vigier**[c], **Neeraj Sinha**[a,*]

[a]Centre of Biomedical Research, SGPGIMS Campus, Raebarelly Road, Lucknow – 226014, INDIA

[b]Department of Chemistry, Institute of Sciences, Banaras Hindu University, Varanasi – 221005, INDIA

[c]National High Magnetic Field Laboratory, Tallahassee, Florida 32304, USA

Abstract

Structural stability of various collagen containing biomaterials such as bones and cartilage is still a mystery. Despite spectroscopic development of several decades, the detailed mechanism of collagen interaction with citrate in bones and glycosaminoglycans (GAGS) in cartilage extracellular matrix (ECM) in its native state is unobservable. We present a significant advancement to probe the collagen interactions with citrate and GAGSin ECM of native bone and cartilage along with specific/non-specific interactions inside collagen assembly at the nanoscopic level through natural abundance dynamic nuclear polarization (DNP) based solid-state nuclear magnetic resonance (ssNMR) spectroscopy. The detected molecular level interactions between citrate – collagen and glycosaminoglycan (GAGs) - collagen inside the native bone and cartilage matrix and other backbone and side-chain interactions in the collagen assembly are responsible for the structural stability and other biomechanical properties of these important class of biomaterial.

Graphical Abstract

[*]Author to whom correspondence should be addressed. neerajcbmr@gmail.com, neeraj.sinha@cbmr.res.in.

Author Contributions

Nidhi Tiwari and Neeraj Sinha conceived and designed the analysis. Sungsool Wi and Frederic Mentink-Vigier collected the data. Nidhi Tiwari and Neeraj Sinha analyzed and interpreted the data. Nidhi Tiwari, Neeraj Sinha drafted the article. Sungsool Wi andFrederic Mentink-Vigier critically revised the article. All the authors have accepted the responsibility for the entire content of the submitted manuscript and approved submission.

Conflicts of interest

There are no conflicts of interest.

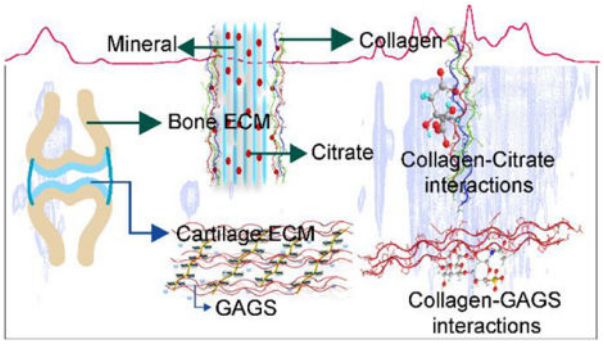

1. Introduction

Higher vertebrates' skeleton is made up of a highly specialized form of connective tissue consisting of bone and cartilage.[1] These connective tissues are primarily composed of fibrous extracellular matrix (ECM), involved in diverse physiological roles, including nutrient storage, endocrine function, and providing structural integrity.[2] Collagen is the most abundant structural component in the extracellular matrix of these connective tissues, which forms a scaffold to provide strength and structure,known for itswide range of functions, including local storage, entrapment, delivery of growth factors, tissue morphogenesis, and tissue repair.[3,4] The most common natural occurrence in all connective tissue and a broad range of functional behaviormake it a widely studied biological system. Most of the studies had been done using extracted collagen, model peptide, and molecular dynamic simulation.[5–7] The absolute native environment of collagen in connective tissues is formed with other ECM components and interactions among them, hence responsible for different structural arrangements than the extracted form of collagen.[8]The collagen protein poses a triple helical structure, which is a polypeptide chain primarily consist of a unique amino acid sequence of glycine (Gly), proline (Pro), and hydroxyproline (Hyp) as repeating units.[9] The triple-helical fibrillar structure of collagen is stabilized by water-mediated hydrogen bonds and stereo-electric effect of Hyp ring,which endorse the non-specific self-association along with charged and hydrophobic interactions, which confer specificity and a high affinity for self-association.[10–15] The structural and functional role, along with unique biomechanical properties of these connective tissues, including load-bearing capacity, tensile and shear strength, and shock absorption, are directly governed by collective intra- and intermolecular interactions between its ECM components. Mapping these interactions at the atomic level in native bone and cartilage can provide better insights into their working mechanism.[16]

Bone mineralization is a crucial step in bone formation. Collagen present in boneprovides a template for the deposition of calcium phosphate (CaP) and promotes the self-assembly of thesmall amorphous CaP,and other bone ECM components such as water and lipid are essential to manifest the process.[17–20] Citrate is an abundant structural component of bone ECM, constituting 1–5% weight of bone organic matrix[21], has a high binding affinity to the calcium stored in hard tissue, plays a pivotal role in regulating metabolic function, and maintaining the structural integrity of the bone.[22] Citrate plays a significant role in improving the mineralization of collagen by facilitating the intrafibrillar formation of

hydroxyapatite (HAP).[23,24] Besides, citrate has been widely used as a medical drug in osteoporosis, and vitamin-D deficient rickets disease is treated with vitamin-D and citrate therapy.[25]Recent NMR/X-ray studies of bone have identified that citrate is a bound component of apatite nanocrystal/collagen complex and acts as a bridging element between the layers of mineral platelets of bone.[24,26,27] Reynolds et al. performed a study that revealed the existence of two distinct pools of citrate in bone ECM. One pool (~65–80% of the total citrate) is associated with the hydroxyapatite component, while another pool (~20–35% of the total citrate) is tightly bound to the collagen component of the apatite nanocomposite-collagen complex, detected by wet chemical analysis.[28] Citrate bound with HAP is a well-studied phenomenon, while the interaction of citrate with collagen at the molecular/atomic level in native bone ECM has not been well defined.

In cartilage ECM, high water content combined with a fibrillar portion (collagen and proteoglycan) provides the load-bearing capacity to the cartilage and enables the low frictional movement to the joints.[29] The ECM of cartilage is made up of type II collagen protein (~12 wt.%), proteoglycan (~6 wt. %), and water (~ 82 wt.%). The polysaccharides chains of proteoglycan consist of chondroitin sulfate (CS), a major component, keratan sulfate (KS), and hyaluronan.[30–32]Proteoglycan glycosaminoglycans (GAGS)-collagen interactions contribute not only to cartilage biomechanics but are also essential to governing the chondrocyte activities and ECM assembly.[33–36] Few studies in the literature that identifies the direct, non-specific interactions between the proteoglycan GAGS and the fibrillar collagen network in cartilage ECM had been reported. Therefore, studying the interaction between two primary constituents of cartilage ECM is essential to understand the cartilage tissue function and associated diseases.

Due to the complex heterogeneous structure of cartilage and bone ECM, it is quite challenging for most of the biophysical techniques to investigate such biological systems at the atomic level in their native state. Solid-state nuclear magnetic resonance (ssNMR) is a well-established and non-destructive technique capable of studying the complex heterogeneous morphology of bone and cartilage ECM in their native state.[37,38] Despite advancements in ssNMR instrumentation and methodologies, the low sensitivity must often be compensated by isotopic enrichment. This severely limits the applicability of all these ssNMR methods for atomic-level investigation of different components of bone and cartilage ECM, where natural isotopic abundance is the main viable approach. Recent advancements in ssNMR instrumentation and methodology had solved the problem of sensitivity enhancement to some extent. The ^{1}H-detected NMR measurements under ultrafast MAS (>60 kHz) conditions[39,40] led to an improvement in spectral resolution of ^{1}H detected lines shapes and sensitivity enhancement in bone spectraby suppressing the ^{1}H–^{1}H homonuclear dipolar couplings and other ^{1}H anisotropic interactions, responsible for line broadening in the ^{1}H NMR spectra. In addition, recently developed biosolid CryoProbe, facilitated us to get 3–4 folds sensitivity enhancement in bone spectra[41,42] at natural isotopic abundance. The sensitivity gain with both the techniques is not enough for detecting the interaction among the various constituents in bone and cartilage ECM in their native state. In this context, MAS-Dynamic Nuclear Polarization (MAS-DNP)[43–47]is an excellent technique to alleviate the inherently low sensitivity of MAS-ssNMR towards the non-isotopically labeled ECM of bone and cartilage in their native state.

In the present study, we have employed MAS-DNP enhanced ssNMR methods to the native bone and cartilage sample to probe the nanoscopic length structure along with associated interactions of both ECM by utilizing DNP based 2D ^{1}H-^{13}C/^{15}N heteronuclear correlation HETCOR and ^{13}C-^{13}C double quantum (DQ)-single quantum (SQ) NMR experiments in natural abundance.[48–51] With the help of these experiments, we were able to probe the collagen-citrate (bone ECM) and collagen-GAGS (cartilage ECM) molecular interactions along with other non-specific and specific interactions present in the collagen assembly at natural isotopic abundance. These interactions are responsible for the structural stability of these important classes of biomaterials.

2. Experimental section

2.1. MAS- DNP sample preparation

All the DNP-ssNMR experiments were performed on the cortical femora bone and articular cartilage of Goat (Capra hircus, 2–3 years old). After cleaning, small pieces of full-thickness cartilages were carefully removed from bones by the scalpel, and small-sized flakes of bone were obtained by filing the intact bone with the help of a scalpel. About 60 mg of each sample (powdered bone and cartilage tissue sample) was mixed with 60 μL of nitroxide biradical AMUPOL[52] 10 mM in 90% D_2O and 10% H_2O in an Eppendorf tube for thorough mixing. The sample mixture was packed into a 3.2 mm thin-walled zirconia rotor with a vessel cap for low–temperature experiments.

2.2. MAS-DNP-ssNMR parameters:

MAS-DNP solid-state NMR spectra were obtained on a wide-bore 600 MHz Bruker Avance III spectrometer equipped with a 395 GHz gyrotron microwave source by employing a 3.2 mm MAS ^{1}H-^{13}C-^{15}N triple-resonance Bruker probe.[53] The sample temperature for DNP experiments under magic-angle spinning (MAS) condition was maintained at about 100 K by flowing nitrogen gas stream to the sample compartment as well as to the bearing and drive inlets of the MAS controller unit for MAS spinning at $\nu_r = 8$ kHz. The nitrogen gas stream used for both variable temperature control and the MAS spinning regulation was obtained by evaporation from a liquid nitrogen tower and was fed into the system through the DNP cabinet with an appropriate set of regulations. A saturation recovery pulse sequence was placed along the proton channel before each NMR pulse sequence with an optimal build–up time of about 10 s, while the microwave is continuously irradiated at the sample with appropriate power. The DNP enhancement factors observed in our ^{1}H-^{13}C and ^{1}H-^{15}N CPMAS experiments were about $\varepsilon = 30$ and $\varepsilon = 30$, respectively. The ^{1}H and ^{13}C 90-degree pulses used were 2.5 μs and 3.5 μs, respectively, for all experiments. The ^{1}H-^{13}C and ^{1}H-^{15}N CPMAS pulse parameters employed were $\nu_{1H} = 60\pm5$ kHz, $\nu_{13C} = 50\pm5$ kHz for 1 ms and $\nu_{1H} = 35\pm5$ kHz, $\nu_{15N} = 25\pm5$ kHz for 1.5 ms, respectively, by employing a ramped (90%–110%) spin-lock pulses along the ^{1}H channel while simultaneously applying a rectangular spin-lock pulse either on ^{13}C or ^{15}N. The basic pulse unit of the PMLG consists of $\{(P)_5(P)_5\}_n$. The ^{1}H pulse power used during the PMLG mixing was 100 kHz. Thus, the width of the basic pulse unit P is 1.41 μs with $n = 1$. For acquiring a 2D ^{1}H-X (X = ^{13}C or ^{15}N) HETCOR spectrum, the dwell time of the indirect time domain was set to $\{(P)_5(P)_5\}_2$ with $n = 2$, which is 28.2 μs.The pulse power of the SPC-5 sequence block for the ^{13}C-^{13}C

2D INADEQUATE[54] experiment was $\nu_{13C} = 5\nu_r = 40$ kHz and ν_{1H}= 110 kHz. Typically, 512 and 4096 scans were acquired for obtaining a noise-free 1-dimensional (1D) ^{1}H–^{13}C and ^{1}H-^{15}N CPMAS spectrum, respectively. For obtaining 2D ^{1}H-^{13}C HETCOR[55] and ^{13}C-^{13}C INADEQUATE experiments, 256 t_1 slices were acquired with 64 scans for each t_1 slice. For obtaining a 2D ^{1}H-^{15}N HETCOR experiment, 256 t_1 slices were acquired with 256 scans for each t_1 slice. SPINAL-64[56] proton decoupling sequence was used during the direct acquisition period, with a 100 kHz decoupling power. Gaussian window function was used for processing the 1D ^{1}H–^{13}C and ^{1}H-^{15}N CPMAS, 2D ^{1}H-^{13}C/^{15}N HETCOR, and ^{13}C-^{13}C INADEQUATE spectra.

3. Results and discussion

3.1. Enhanced resonances from citrate, GAGS, and aromatic amino acid residues inside the bone and cartilage matrix:

Collagen is an integral part of both bone and cartilage ECM. The DNP enhanced 1D ^{1}H-^{13}C CPMAS spectrum of collagen protein in native bone shows ~ 30 - fold sensitivity enhancement in ^{13}C resonances when the microwave is ON (Figure.S1(A)) over that when the microwave is OFF (Figure.S1(B)). We have assigned most of the ^{13}C resonances from the organic matrix in native bone and cartilage ECM (Figure.1A and 1B) as per the reported literature.[8,38,57] Observed ^{13}C resonances from the backbone of collagen protein, including Gly, Pro, and Hyp, are similar to the spectrum recorded with conventional ssNMR methods, suggesting that structural integrity of the organic matrix remains unaffected even at low temperature and doping with biradical. Aliphatic residues predominantly dominate the 1D ^{1}H-^{13}C CPMAS spectra of collagen. However, a significant signal enhancement is observed in ^{13}C resonances from citrate (74 – 76 ppm), aromatic amino acid (AAs) residues (Phe, Tyr, His at 129 ppm), and Arg Cζ (156.8 ppm) of collagen protein,whichhave extremely low abundance in the bone ECM. Similarly, in the cartilage matrix, signal enhancement is observed in ^{13}C resonances from GAGS ring carbons (103.6, 84, 76, 79 ppm), aromatic residues (129 ppm), and Arg Cζ (156.8 ppm).[58]The complex heterogeneous structure of cartilage ECM consists of highly mobile GAGS and relatively rigid collagen protein, a line broadening in a few of ^{13}C resonances is observed. A dominating factor that governs the linewidths of DNP spectra is the formation of a glassy state of the sample under the frozen condition (~ 100 K) due to the mixing with the DNP juice. Then, a glassy, disordered sample state resulted in, would increase the heterogeneity of the sample and conformation that results in forming a slightly asymmetric peak shape, Czjzeklineshape (figureS8), as shown in the 2D ^{1}H-^{13}C DNP HETCOR spectrum of cartilage sample. The major peak around 7 ppm in the projected ^{1}H spectrum shown on the left in red color, is taken as a projection from 57 ppm to 60 ppm along ^{13}C, exhibits the characteristic Czjzek lineshape,[59,60] an asymmetric lineshape that results due to the formation of a disordered glassy sample state. In this DNP sample condition, the linewidths coming from the sample's intrinsic heterogeneity in the conformation would be much less than that from the formation of a glassy state after freezing the sample that is mixed with the DNP juice. Under our DNP sampling condition, the paramagnetic contribution to the line widths of the peaks is negligible.

Overall, an increase in signal intensity of ^{13}C resonances from the molecules which are present in extremely low concentration in the matrix of both cartilage and bone facilitates us to record more advanced DNP-based ssNMR experiments.

3.2. High-resolution structural insights into the native bone and cartilage ECM:

Native collagen and extracted collagen have been extensively studied using ssNMR[5,37,57], but its interactions with low abundant components such as citrate and GAGS in native bone and cartilage ECM could not have been depicted due to the limited applicability of ssNMR in natural abundance. Thereforeto probe the molecular interactions between collagen and other ECM components of native bone and cartilage, we performed MAS-DNP based 2D PMLG ^{1}H-^{13}C HETCORexperiments in natural abundance at a cross-polarization (CP) contact time 200 μs. At 100 μs contact time, 2D PMLG ^{1}H-^{13}C HETCOR spectra gave identical results but with a poor signal to noise ratio (SNR). Intermolecular correlations areobserved among various constituents,which are ^{1}H-^{13}C dipolar coupled in their spatial proximity. In bone ECM, we majorly focused on probing the molecular interactions between citrate and collagen.

Citrate, having three carboxylate groups, is synthesized and produced by osteoblast during bone formation.[28] The major citrate's pool is strongly associated with hydroxyapatite (HAP), while ~ 20–35% citrate is tightly bound to collagen. The molecular association of citrate with collagen protein at the atomic level is observed in the 2D ^{1}H-^{13}C HETCOR spectrum of the bone sample in natural isotopic abundance. Various molecular interactions in native bone ECM are shown in Figure.2. The chemical structure of the citrate molecule is shown in Figure S3. The citrate chemical shift at 75.8 ppm corresponds to the quaternary carbon of citrate, and protons associated with citrate appear at 2.7 ppm–3.5 ppm. Hence correlation of quaternary carbon of citrate with collagen residues is due to ^{1}H-^{13}C dipolar coupling networks, which are in spatial proximity. The ^{1}H and ^{13}C slices of the cross peak of interest from the 2D ^{1}H-^{13}C HETCOR spectrum of bone are given in Figure S4. Molecular interaction between citrate (75.8 ppm) and protons of Aromatic AAs ring carbons (Phe, Tyr, Trp, His at 129 ppm) is observed (Figure.2A), showing citrate is involved in hydrophobic interaction with Aromatic AAs of collagen protein. Besides this, citrate shows molecular interaction with the charged residue of collagen protein, including protons of Arg Cβ (34.6 ppm) and Glu Cγ (31.6 ppm), as shown in Figure.2B, suggesting the existence of charge-pair interactions and hydrogen bonding between them. The correlation of protons of Ala Cα (48.2 ppm) and Ala Cβ (19.6 ppm) from collagen protein with citrate shows a non-covalent association with citrate molecules. These findings suggest that collagen protein in bone ECM may involve in citrate homeostasis in the bone metabolic pathway. Besides the collagen-citrate interactions, long-range interactions are seen between Aromatic AAs ring carbons and the carboxylate group of acidic amino acid residues such as Glu/Asp. Hydrogen bonding network, as well as some hydrophobic interactions, were observed in the collagen matrix (Figure.2).

The structural-functional mechanism of cartilage tissue is determined by its hierarchical structure along with collagen-proteoglycan biomechanical properties derived from the nanoscale level. Study of the atomic-scale structure and associated interactions in native

cartilage ECM guides in understanding the mechanism of degenerative cartilage diseases such as osteoarthritis, which starts with the fragmentation of proteoglycans followed by disruption of the collagen network leads to cartilage loss.[61,62] The polysaccharide unit (GAGS) of proteoglycan plays a predominant role in cell signaling, development, angiogenesis, and cell proliferation.[35] Therefore, to probe the collagen-GAGS correlation in native cartilage ECM at the atomic-level, we performed a 2D PMLG ^{1}H-^{13}C HETCOR experiment employing a CP contact time 200 μs. A 2D ^{1}H-^{13}C HETCOR spectrum (Figure.3) shows the correlation between the resonances of GAGS and collagen residues. The chemical structure of the monomeric unit of GAGS (chondroitin sulfate) is shown in figure S3. Well-resolved resonances observed between 95–107 ppm are arising from α and β GAGS C1 carbons. The proton chemical shift for C1 of GAGS appears at 4.5 ppm–5.5 ppm, and for C5, it lies between 3.4 ppm–4.0 ppm as per literature.[58,63] GAGS carbons are correlated with collagen protein residues through ^{1}H-^{13}C dipolar coupling networks, which are in spatial proximity. The ^{13}C and ^{1}H slices of the cross peak of interest from the 2D ^{1}H-^{13}C HETCOR spectrum of cartilage are given in Figures S5A and 5B. GAGS C1 (103 ppm) resonance shows a correlation with protons of Hyp Cγ (71 ppm), Arg Cα (54.5 ppm), Ala Cα (49.2), and Hyp Cβ (38.5 ppm). Correlation between GAGS C1 (96.3 ppm) and Gly Cα (43 ppm) is observed. Similarly, GAGS C1 resonances at 102.5 ppm and 100.7 ppm show interaction with Ala Cα (49.2 ppm), Lys Cβ (35.8 ppm), Arg Cβ (29.6 ppm), Lys Cα (56.5 ppm), Asp Cα (50.8 ppm), and Lys Cε (40.2 ppm) through ^{1}H-^{13}C dipolar coupling networks, respectively as represented in Figure.3. Besides this, resonance at 116 ppm arising from protons of Trp Cζ1/Tyr Cε1 shows a correlation with GAGS C5 (76.5 ppm). In a broader picture, GAGS ring carbon resonances show molecular interactions with Hyp, Arg, Lys, Asp, Gly, along with Trp/Tyr ring carbons. The negatively charged GAGS unit forms charge-pair salt-bridge type interaction with positively charged residues Arg/Lys of collagen protein,[64] while Hyp and Asp may involve in hydrogen bonding with GAGS. Interaction of GAGS with aromatic residues suggests the existence of CH-π type interactions. The position and interactions between proteoglycan-GAGS and collagen fibrils are not fixed; they can conceivably break and reform reversibly.[65,66] This unique property provides flexibility and cushioning to the cartilage tissue against applied mechanical stress. Apart from GAGS-collagen interactions, we observed many non-specific (Hydrogen bonding) and specific (hydrophobic and charged) interactions inside the collagen supra-assembly, as shown in Figure.3.

Further, to map the structural integrity of collagen protein inside the bone and cartilage ECM through the ^{13}C-^{13}C homonuclear dipolar coupling network, we performed the SPC5 experiment to obtain ^{13}C DQ-^{13}C SQ correlation spectra by spinning samples at 8 kHz MAS rate [$\nu_{rf}(^{13}C)$=40 kHz] while employing a contact time of 1000 μs.[67,68] Figures.4A and 4B show the ^{13}C DQ-^{13}C SQ spectra of bone and cartilage ECM in natural isotopic abundance. In the ^{13}C DQ-SQ spectra of both ECM, short (one bond) and long-range correlation (more than one bond) are observed. The ^{13}C DQ-^{13}C SQ spectrum indicates the ^{13}C-^{13}C correlation arising from collagen protein resonances. A ^{13}C DQ-^{13}C SQ correlation between Aromatic AAs ring carbons-Aromatic AAs Cα and Arg Cζ– Carbonyl carbon along with correlation among the aliphatic residues of collagen protein in the ECM of cartilage indicating that the ^{13}C-^{13}C dipolar coupling network in both the ECM is different from each

other. The ^{13}C DQ-^{13}C SQ experiments are useful in probing the structural difference in collagen assembly because it enables mapping of ^{13}C polarization transfer through space inside the ECM of bone and cartilage in their native state.

3.3. Probing backbone and side-chain interactions inside native collagen assembly:

Due to very low occurrence (0.37%) and low gyromagnetic ratio (-2.7126×107 rad $T^{-1}s^{-1}$) of ^{15}N nuclei, acquiring ^{15}N spectra of collagen protein in natural isotopic abundance is beyond the ssNMR detection limits.[69] Therefore, to probe the backbone structure along with side chains of other basic residues (Arg, Lys) of native collagen protein in bone and cartilage matrix without ^{15}N labeling, we have utilized the DNP based ^{15}N-ssNMR experiments. The 1D ^{1}H-^{15}N CPMAS spectra of bone and cartilage matrix are shown in Figure.5A and 5C. In the 1D ^{1}H-^{15}N CPMAS spectrum of bone (Figure.5A), we have assigned the resonances exclusively from Gly N (109.2 ppm), Hyp/Pro N (129.9 ppm), Arg Nε (82.5ppm), Arg Nη(71.0 ppm), Lys Nζ (38 ppm and 31.7 ppm) and Trp Nε (138 ppm). Similarly, the resonances exclusively from Gly N (109.2 ppm), Hyp/Pro N (129.8 ppm), Arg Nε (82.3 ppm), Arg Nη(71.3 ppm), Lys Nζ (37.1 and 29.1 ppm), and Trp Nε (138 ppm) are assigned for the 1D ^{1}H-^{15}N CPMAS spectrum of cartilage (Figure.5C).[70,71] In both matrices, ^{15}N resonances from collagen protein are observed at nearly the same chemical shift except Lys Nζ (38 and 31.7 ppm), evidencing a different chemical environment around Lys residue. Remarkable sensitivity enhancement in natural abundance 1D ^{1}H-^{15}N CPMAS spectra directs us to record further the 2D ^{1}H-^{15}N HETCOR spectra of both samples. The 2D PMLG ^{1}H-^{15}N HETCOR spectra reveal a different molecular arrangement of the backbone and side-chain residues in collagen assembly inside bone and cartilage matrices (Figure.5B and 5D). The ^{15}N slices of the cross peak of interest from the 2D ^{1}H-^{15}N HETCOR spectrum of cartilage are given in Figure S6. In Figure.5B, the molecular interactions between protons of Arg Nε - His N/Asp N (119.9 ppm), Arg Nε-Thr N, and Arg Nε-Gly N are observed through ^{1}H-^{15}N dipolar coupling network in the spatial proximity of collagen assembly. Arg side-chains form cation-π interactions with aromatic amino acid and cation pair interactions with the acidic amino acid in collagen protein. A Correlation between protons of Pro/Hyp N and Trp Nε is observed. It has been reported earlier that Pro/Hyp shows CH-π interactions with aromatic amino acids. These hydrophobic interactions, including cation–π, CH-π and cation-pair, add specificity and extra stability to the higher-order structure of collagen protein. The 2D ^{1}H-^{15}N HETCOR spectrum from cartilage ECM shows different molecular interactions from the bone ECM. A correlation is observed betweenPro/Hyp N –Gly N, showing these residues are involved in interstrand hydrogen bonding in collagen protein. Molecular interactions between protons of Trp Nε-Gln N, Arg Nε- Lys Nζ, and Arg Nη-Lys Nζ are observed. The intra-molecular Arg-Lys residues are involved in the advanced glycation end product (AGE) cross-linking sites in collagen protein.[72] The properties of collagenous tissues are adversely affected by the formation of AGE. Besides this, they are even linked to the presence of several age-related disorders.[72] Thus, probing molecular interaction through the 2D ^{1}H-^{15}N HETCOR experiment may help elucidate the structural disorders associated with disease conditions in bone and cartilage.

The huge gain in sensitivity, makes DNP-MAS ssNMR methods preferable in elucidating the structure details of such complex heterogeneous systems. In the process of acquiring

MAS-DNP ssNMR spectra, some challenges were faced. In sample preparation, The size of the powder particles, particularly in the case of the cartilage samples, is relatively large that the size of a single particle can reach tens to hundreds of micrometers in diameter. Thus, rather than obtaining a spectrum evenly for the entire sample particle, the surface of the particle that is close to DNP juice would be over sampled. This limitation can be reduced by making the sample into smaller granular powder or by penetrating the radicals in DNP juice deeper into the core of the sample particle if the matrix of sample possesses porous pores. In addition, a line broadening effect is also seen in cartilage spectra, which is associated with the DNP sampling condition for making a glassy state, which causes the disorderedness of the molecular association that makes an asymmetrically broadened line shape (Czjzek line shape).

4. Conclusion

Natural abundance ssNMR experiments are challenging for elucidating the structural details of the complex heterogeneous biomaterial such as bone and cartilage, but the impressive gains in sensitivity realized with MAS-DNP facilitate us to perform the 2D ^{1}H-^{15}N, ^{1}H-^{13}C HETCOR, and ^{13}C DQ-^{13}C SQ experiments. With the help of these experiments, we were able to probe the Collagen-citrate (bone ECM) and collagen-GAGS (cartilage ECM), along with the other molecular interactions in collagen protein assembly in both the ECM. From 2D ^{1}H-^{13}C HETCOR, it was depicted that citrate shows molecular interactions with Arg, Glu Ala, and Aromatic AAs residues of collagen protein inside bone matrix. These findings confirmed that citrate is an integral component of apatite-collagen nanocomposite in bone matrix. Similarly, the direct interactions of GAGS resonances with Hyp, Arg, Lys, Asp, Gly, along with Trp/Tyr resonances of collagen protein inside cartilage ECM were observed in 2D ^{1}H-^{13}C HETCOR spectrum, indicating that GAGS molecules involved in ionic and non-ionic such as hydrogen bonds and hydrophobic interactions with amino acid residues of collagen protein, responsible for the stability of cartilage ECM and their physiochemical properties. We differentiated the structural assembly of collagen by mapping the ^{13}C -^{13}C dipolar coupling network in both the ECM. Additionally, utilizing the 2D ^{1}H-^{15}N HETCOR experiments in natural abundance, which were not possible earlier without DNP, gave insights into the backbone and side-chain structural map of collagen matrix inside bone and cartilage. The structural studies, along with molecular interaction in bone and cartilage ECM, would be helpful in comprehending the structural-functional mechanism and their biomechanical properties, thus provides guidance in the development of prevention and care therapy for the diseases which are associated with bone and cartilage disorders.

Overall, the impressive gain in sensitivity encourages the possibility of performing DNP enhanced ^{13}C-^{13}C as well as ^{13}C-^{15}N correlation, REDOR/RR types experiments, and various other 3D experiments to elucidate the 3D structural details in the absolute native environment of bone and cartilage at natural isotopic abundances.

Supplementary Material

Refer to Web version on PubMed Central for supplementary material.

Acknowledgments

The authors gratefully acknowledge SERB (EMR/2015/001758), the Council of Scientific and Industrial Research (CSIR), India, for financial support. The authors are also thankful to the National High Magnetic Field Laboratory, Tallahassee, Florida, which is supported by the NIH P41 GM122698, NIH S10 OD018519, and National Science Foundation Cooperative Agreement No. DMR-1644779. We also acknowledge Prof. RamaNand Rai and Navneet Dwivedi for their valuable suggestions and help.

References

(1). Hall BK Bones and Cartilage: Developmental and Evolutionary Skeletal Biology: Second Edition; Elsevier Inc., 2015. 10.1016/C2013-0-00143-0.

(2). McKee TJ; Perlman G; Morris M; Komarova SV Extracellular Matrix Composition of Connective Tissues: A Systematic Review and Meta-Analysis. Sci. Rep 2019, 9 (1), 1–15. 10.1038/s41598-019-46896-0. [PubMed: 30626917]

(3). Shoulders MD; Raines RT Collagen Structure and Stability. Annu. Rev. Biochem 2009, 78 (1), 929–958. 10.1146/annurev.biochem.77.032207.120833. [PubMed: 19344236]

(4). Gelse K; Pöschl E; Aigner T Collagens - Structure, Function, and Biosynthesis. Adv. Drug Deliv. Rev 2003, 55 (12), 1531–1546. 10.1016/j.addr.2003.08.002. [PubMed: 14623400]

(5). Bella J; Eaton M; Brodsky B; Berman H Crystal and Molecular Structure of a Collagen-like Peptide at 1.9 A Resolution. Science (80-.) 1994, 266 (5182), 75–81. 10.1126/science.7695699.

(6). Aliev AE; Courtier-Murias D Water Scaffolding in Collagen: Implications on Protein Dynamics as Revealed by Solid-State NMR. Biopolymers 2014, 101 (3), 246–256. 10.1002/bip.22330. [PubMed: 23784805]

(7). Fu I; Case DA; Baum J Dynamic Water-Mediated Hydrogen Bonding in a Collagen Model Peptide. Biochemistry 2015, 54 (39), 6029–6037. 10.1021/acs.biochem.5b00622. [PubMed: 26339765]

(8). Rai RK; Singh C; Sinha N Predominant Role of Water in Native Collagen Assembly inside the Bone Matrix. J. Phys. Chem. B 2015, 119 (1), 201–211. 10.1021/jp511288g. [PubMed: 25530228]

(9). Rich A; Crick FHC The Molecular Structure of Collagen. J. Mol. Biol 1961, 3 (5), 483–506. 10.1016/S0022-2836(61)80016-8. [PubMed: 14491907]

(10). Jenkins CL; Raines RT Insights on the Conformational Stability of Collagen. Nat. Prod. Rep 2002, 19 (1), 49–59. 10.1039/a903001h. [PubMed: 11902439]

(11). Singh C; Rai RK; Aussenac F; Sinha N Direct Evidence of Imino Acid-Aromatic Interactions in Native Collagen Protein by DNP-Enhanced Solid-State NMR Spectroscopy. J. Phys. Chem. Lett 2014, 5 (22), 4044–4048. 10.1021/jz502081j. [PubMed: 26276492]

(12). Chen CC; Hsu W; Hwang KC; Hwu JR; Lin CC; Horng JC Contributions of Cation-π Interactions to the Collagen Triple Helix Stability. Arch. Biochem. Biophys 2011, 508 (1), 46–53. 10.1016/j.abb.2011.01.009. [PubMed: 21241657]

(13). Kar K; Ibrar S; Nanda V; Getz TM; Kunapuli SP; Brodsky B Aromatic Interactions Promote Self-Association of Collagen Triple-Helical Peptides to Higher-Order Structures. Biochemistry 2009, 48 (33), 7959–7968. 10.1021/bi900496m. [PubMed: 19610672]

(14). Bella J; Berman HM Crystallographic Evidence for Cα–H···O=C Hydrogen Bonds in a Collagen Triple Helix. J. Mol. Biol 1996, 264 (4), 734–742. 10.1006/jmbi.1996.0673. [PubMed: 8980682]

(15). Fallas JA; Dong J; Tao YJ; Hartgerink JD Structural Insights into Charge Pair Interactions in Triple Helical Collagen-like Proteins. J. Biol. Chem 2012, 287 (11), 8039–8047. 10.1074/jbc.M111.296574. [PubMed: 22179819]

(16). Scott JE Proteoglycan-Fibrillar Collagen Interactions. Biochem. J 1988, 252 (2), 313–323. 10.1042/bj2520313. [PubMed: 3046606]

(17). Irving JT Calcification of the Organic Matrix of Enamel. Arch. Oral Biol 1963, 8 (6), 773–774. 10.1016/0003-9969(63)90010-4. [PubMed: 14081617]

(18). Landis WJ; Song MJ; Leith A; McEwen L; McEwen BF Mineral and Organic Matrix Interaction in Normally Calcifying Tendon Visualized in Three Dimensions by High-Voltage Electron

Microscopic Tomography and Graphic Image Reconstruction. J. Struct. Biol 1993, 110 (1), 39–54. 10.1006/jsbi.1993.1003. [PubMed: 8494671]

(19). Bonucci E Fine Structure of Early Cartilage Calcification. J. Ultrastruct. Res 1967, 20 (1–2), 33–50. 10.1016/S0022-5320(67)80034-0. [PubMed: 4195919]

(20). Tiwari N; Rai RN; Sinha N Water-Lipid Interactions in Native Bone by High-Resolution Solid-State NMR Spectroscopy. Solid State Nucl. Magn. Reson 2020, 107, 101666. 10.1016/j.ssnmr.2020.101666. [PubMed: 32371298]

(21). Reid DG; Duer MJ; Jackson GE; Murray RC; Rodgers AL; Shanahan CM Citrate Occurs Widely in Healthy and Pathological Apatitic Biomineral: Mineralized Articular Cartilage, and Intimal Atherosclerotic Plaque and Apatitic Kidney Stones. Calcif. Tissue Int 2013, 93 (3), 253–260. 10.1007/s00223-013-9751-5. [PubMed: 23780351]

(22). Dickens F The Citric Acid Content of Animal Tissues, with Reference to Its Occurrence in Bone and Tumour1. Biochem. J 1941, 35 (8–9), 1011–1023. 10.1042/bj0351011. [PubMed: 16747445]

(23). Shao C; Zhao R; Jiang S; Yao S; Wu Z; Jin B; Yang Y; Pan H; Tang R Citrate Improves Collagen Mineralization via Interface Wetting: A Physicochemical Understanding of Biomineralization Control. Adv. Mater 2018, 30 (8), 1–7. 10.1002/adma.201704876.

(24). Davies E; Müller KH; Wong WC; Pickard CJ; Reid DG; Skepper JN; Duer MJ Citrate Bridges between Mineral Platelets in Bone. Proc. Natl. Acad. Sci. U. S. A 2014, 111 (14). 10.1073/pnas.1315080111.

(25). Norman AW; Deluca HF Vitamin D and the Incorporation of [1-14C]Acetate into the Organic Acids of Bone; 1964; Vol. 91.

(26). Hu YY; Liu XP; Ma X; Rawal A; Prozorov T; Akinc M; Mallapragada SK; Schmidt-Rohr K Biomimetic Self-Assembling Copolymer-Hydroxyapatite Nanocomposites with the Nanocrystal Size Controlled by Citrate. Chem. Mater 2011, 23 (9), 2481–2490. 10.1021/cm200355n.

(27). Hu Y-Y; Rawal A; Schmidt-Rohr K Strongly Bound Citrate Stabilizes the Apatite Nanocrystals in Bone. Proc. Natl. Acad. Sci 2010, 107 (52), 22425–22429. 10.1073/pnas.1009219107. [PubMed: 21127269]

(28). Costello LC; Chellaiah M; Zou J; Franklin RB; Reynolds MA The Status of Citrate in the Hydroxyapatite/Collagen Complex of Bone; and Its Role in Bone Formation. J. Regen. Med. Tissue Eng 2014, 3 (1), 4. 10.7243/2050-1218-3-4. [PubMed: 25745562]

(29). Sophia Fox AJ; Bedi A; Rodeo SA The Basic Science of Articular Cartilage: Structure, Composition, and Function. Sports Health 2009, 1 (6), 461–468. 10.1177/1941738109350438. [PubMed: 23015907]

(30). Ricard-Blum S; Ruggiero F The Collagen Superfamily: From the Extracellular Matrix to the Cell Membrane. Pathol. Biol 2005, 53 (7), 430–442. 10.1016/j.patbio.2004.12.024. [PubMed: 16085121]

(31). Huster D Chapter 4 Solid-State NMR Studies of Collagen Structure and Dynamics in Isolated Fibrils and in Biological Tissues. Annu. Reports NMR Spectrosc 2008, 64, 127–159. 10.1016/S0066-4103(08)00004-5.

(32). Poole AR Proteoglycans in Health and Disease: Structures and Functions. Biochem. J 1986, 236 (1), 1–14. 10.1042/BJ2360001. [PubMed: 3539097]

(33). Heinegård D Proteoglycans and More - From Molecules to Biology. International Journal of Experimental Pathology. 12 2009, pp 575–586. 10.1111/j.1365-2613.2009.00695.x. [PubMed: 19958398]

(34). Y. JH; H. J Tendon Proteoglycans: Biochemistry and Function. J. Musculoskelet. Neuronal Interact 2005, 5 (1), 22–34. [PubMed: 15788868]

(35). Gandhi NS; Mancera RL The Structure of Glycosaminoglycans and Their Interactions with Proteins. Chem. Biol. Drug Des 2008, 72 (6), 455–482. 10.1111/j.1747-0285.2008.00741.x. [PubMed: 19090915]

(36). Rojas FP; Batista MA; Lindburg CA; Dean D; Grodzinsky AJ; Ortiz C; Han L Molecular Adhesion between Cartilage Extracellular Matrix Macromolecules. Biomacromolecules 2014, 15 (3), 772–780. 10.1021/bm401611b. [PubMed: 24491174]

(37). Mroue KH; Viswan A; Sinha N; Ramamoorthy A Solid-State NMR Spectroscopy: The Magic Wand to View Bone at Nanoscopic Resolution, 1st ed.; Elsevier Ltd., 2017; Vol. 92. 10.1016/bs.arnmr.2017.04.004.

(38). Xu J; Zhu P; Morris MD; Ramamoorthy A Solid-State NMR Spectroscopy Provides Atomic-Level Insights into the Dehydration of Cartilage. J. Phys. Chem. B 2011, 115 (33), 9948–9954. 10.1021/jp205663z. [PubMed: 21786810]

(39). Mroue KH; Nishiyama Y; Kumar Pandey M; Gong B; McNerny E; Kohn DH; Morris MD; Ramamoorthy A Proton-Detected Solid-State NMR Spectroscopy of Bone with Ultrafast Magic Angle Spinning. Sci. Rep 2015, 5, 1–10. 10.1038/srep11991.

(40). Singh C; Rai RK; Kayastha AM; Sinha N Ultra Fast Magic Angle Spinning Solid - State NMR Spectroscopy of Intact Bone. Magn. Reson. Chem 2016, 54 (2), 132–135. 10.1002/mrc.4331. [PubMed: 26352739]

(41). Hassan A; Quinn CM; Struppe J; Sergeyev IV; Zhang C; Guo C; Runge B; Theint T; Dao HH; Jaroniec CP et al. Sensitivity Boosts by the CPMAS CryoProbe for Challenging Biological Assemblies. J. Magn. Reson 2020, 311, 106680. 10.1016/j.jmr.2019.106680. [PubMed: 31951864]

(42). Tiwari N; Wegner S; Hassan A; Dwivedi N; Rai R; Sinha N Probing Short and Long-Range Interactions in Native Collagen inside the Bone Matrix by BioSolids CryoProbe. Magn. Reson. Chem 2020. 10.1002/mrc.5084.

(43). Hall DA; Maus DC; Gerfen GJ; Inati SJ; Becerra LR; Dahlquist FW; Griffin RG Polarization-Enhanced NMR Spectroscopy of Biomolecules in Frozen Solution. Science (80-.) 1997, 276 (5314), 930–932. 10.1126/science.276.5314.930.

(44). Hediger S; Lee D; Mentink-Vigier F; De Paëpe G MAS-DNP Enhancements: Hyperpolarization, Depolarization, and Absolute Sensitivity. eMagRes 2018, 7 (4), 105–116. 10.1002/9780470034590.emrstm1559.

(45). Kundu K; Mentink-Vigier F; Feintuch A; Vega S DNP Mechanisms. eMagRes 2019, 8 (3), 295–338. 10.1002/9780470034590.emrstm1550.

(46). Lee D; Hediger S; De Paëpe G Is Solid-State NMR Enhanced by Dynamic Nuclear Polarization? Solid State Nuclear Magnetic Resonance. Elsevier 4 1, 2015, pp 6–20. 10.1016/j.ssnmr.2015.01.003.

(47). Yamamoto K; Caporini MA; Im SC; Waskell L; Ramamoorthy A Cellular Solid-State NMR Investigation of a Membrane Protein Using Dynamic Nuclear Polarization. Biochim. Biophys. Acta - Biomembr 2015, 1848 (1), 342–349. 10.1016/j.bbamem.2014.07.008.

(48). Kang X; Kirui A; Dickwella Widanage MC; Mentink-Vigier F; Cosgrove DJ; Wang T Lignin-Polysaccharide Interactions in Plant Secondary Cell Walls Revealed by Solid-State NMR. Nat. Commun 2019, 10 (1), 1–9. 10.1038/s41467-018-08252-0. [PubMed: 30602773]

(49). Rossini AJ; Zagdoun A; Hegner F; Schwarzwälder M; Gajan D; Copéret C; Lesage A; Emsley L Dynamic Nuclear Polarization NMR Spectroscopy of Microcrystalline Solids. J. Am. Chem. Soc 2012, 134 (40), 16899–16908. 10.1021/ja308135r. [PubMed: 22967206]

(50). Takahashi H; Hediger S; De Paëpe G Matrix-Free Dynamic Nuclear Polarization Enables Solid-State NMR 13C-13C Correlation Spectroscopy of Proteins at Natural Isotopic Abundance. Chem. Commun 2013, 49 (82), 9479–9481. 10.1039/c3cc45195j.

(51). Chow WY; Norman BP; Roberts NB; Ranganath LR; Teutloff C; Bittl R; Duer MJ; Gallagher JA; Oschkinat H Pigmentation Chemistry and Radical-Based Collagen Degradation in Alkaptonuria and Osteoarthritic Cartilage. Angew. Chemie Int. Ed 2020, anie.202000618. 10.1002/anie.202000618.

(52). Sauvée C; Rosay M; Casano G; Aussenac F; Weber RT; Ouari O; Tordo P Highly Efficient, Water-Soluble Polarizing Agents for Dynamic Nuclear Polarization at High Frequency. Angew. Chemie - Int. Ed 2013, 52 (41), 10858–10861. 10.1002/anie.201304657.

(53). Dubroca T; Smith AN; Pike KJ; Froud S; Wylde R; Trociewitz B; McKay J; Mentink-Vigier F; van Tol J; Wi S et al. A Quasi-Optical and Corrugated Waveguide Microwave Transmission System for Simultaneous Dynamic Nuclear Polarization NMR on Two Separate 14.1 T Spectrometers. J. Magn. Reson 2018, 289, 35–44. 10.1016/j.jmr.2018.01.015. [PubMed: 29459343]

(54). Rienstra CM; Jaroniec CP; Hohwy M; Rienstra CM; Jaroniec CP; Griffin RG Fivefold Symmetric Homonuclear Dipolar Recoupling in Rotating Solids: Application To Double Quantum Spectroscopy. Artic. J. Chem. Phys 1999, 110 (16), 7983–7992. 10.1063/1.478702.

(55). Vinogradov E; Madhu PK; Vega S Phase Modulated Lee-Goldburg Magic Angle Spinning Proton Nuclear Magnetic Resonance Experiments in the Solid State: A Bimodal Floquet Theoretical Treatment. J. Chem. Phys 2001, 115 (19), 8983–9000. 10.1063/1.1408287.

(56). Fung BM; Khitrin AK; Ermolaev K An Improved Broadband Decoupling Sequence for Liquid Crystals and Solids. J. Magn. Reson 2000, 142 (1), 97–101. 10.1006/jmre.1999.1896. [PubMed: 10617439]

(57). Rai RK; Sinha N Dehydration-Induced Structural Changes in the Collagen-Hydroxyapatite Interface in Bone by High-Resolution Solid-State NMR Spectroscopy. J. Phys. Chem. C 2011, 115 (29), 14219–14227. 10.1021/jp2025768.

(58). Pomin VH NMR Chemical Shifts in Structural Biology of Glycosaminoglycans. Analytical Chemistry. American Chemical Society 1 7, 2014, pp 65–94. 10.1021/ac401791h.

(59). Ni QZ; Markhasin E; Can TV; Corzilius B; Tan KO; Barnes AB; Daviso E; Su Y; Herzfeld J; Griffin RG Peptide and Protein Dynamics and Low-Temperature/DNP Magic Angle Spinning NMR. J. Phys. Chem. B 2017, 121 (19), 4997–5006. 10.1021/acs.jpcb.7b02066. [PubMed: 28437077]

(60). Takahashi H; Fernández-De-Alba C; Lee D; Maurel V; Gambarelli S; Bardet M; Hediger S; Barra AL; De Paëpe G Optimization of an Absolute Sensitivity in a Glassy Matrix during DNP-Enhanced Multidimensional Solid-State NMR Experiments. J. Magn. Reson 2014, 239, 91–99. 10.1016/j.jmr.2013.12.005. [PubMed: 24480716]

(61). Hardingham T Chondroitin Sulfate and Joint Disease. Osteoarthr. Cartil. Osteoarthr. Res. Soc 1998, 6, 3–5.

(62). Vinatier C; Guicheux J Cartilage Tissue Engineering: From Biomaterials and Stem Cells to Osteoarthritis Treatments. Annals of Physical and Rehabilitation Medicine. Elsevier Masson SAS 6 1, 2016, pp 139–144. 10.1016/j.rehab.2016.03.002.

(63). Toida T; Toyoda H High-Resolution Proton on Chondroitin Sulfates Nuclear Magnetic Resonance Studies; Vol. 9.

(64). Joseph PRB; Sawant KV; Iwahara J; Garofalo RP; Desai UR; Rajarathnam K Lysines and Arginines Play Non-Redundant Roles in Mediating Chemokine-Glycosaminoglycan Interactions. Sci. Rep 2018, 8 (1), 2–11. 10.1038/s41598-018-30697-y. [PubMed: 29311662]

(65). Scott JE Elasticity in Extracellular Matrix “shape Modules” of Tendon, Cartilage, Etc. A Sliding Proteoglycan-Filament Model. Journal of Physiology. 12 1, 2003, pp 335–343. 10.1113/jphysiol.2003.050179. [PubMed: 14766149]

(66). Lewis PN; Pinali C; Young RD; Meek KM; Quantock AJ; Knupp C Structural Interactions between Collagen and Proteoglycans Are Elucidated by Three-Dimensional Electron Tomography of Bovine Cornea. Structure 2010, 18 (2), 239–245. 10.1016/j.str.2009.11.013. [PubMed: 20159468]

(67). Su Y; Hong M Conformational Disorder of Membrane Peptides Investigated from Solid-State NMR Line Widths and Line Shapes. J. Phys. Chem. B 2011, 115 (36), 10758–10767. 10.1021/jp205002n. [PubMed: 21806038]

(68). Hohwy M; Rienstra CM; Jaroniec CP; Griffin RG Fivefold Symmetric Homonuclear Dipolar Recoupling in Rotating Solids: Application to Double Quantum Spectroscopy. J. Chem. Phys 1999, 110 (16), 7983–7992. 10.1063/1.478702.

(69). Gutmann T; Liu J; Rothermel N; Xu Y; Jaumann E; Werner M; Breitzke H; Sigurdsson ST; Buntkowsky G Natural Abundance 15N NMR by Dynamic Nuclear Polarization: Fast Analysis of Binding Sites of a Novel Amine-Carboxyl-Linked Immobilized Dirhodium Catalyst. Chem. - A Eur. J 2015, 21 (9), 3798–3805. 10.1002/chem.201405043.

(70). Goldberga I; Li R; Chow WY; Reid DG; Bashtanova U; Rajan R; Puszkarska A; Oschkinat H; Duer MJ Detection of Nucleic Acids and Other Low Abundance Components in Native Bone and Osteosarcoma Extracellular Matrix by Isotope Enrichment and DNP-Enhanced NMR. RSC Adv. 2019, 9 (46), 26686–26690. 10.1039/c9ra03198g.

(71). Singh C; Sinha N Mechanistic Insights into the Role of Water in Backbone Dynamics of Native Collagen Protein by Natural Abundance 15N NMR Spectroscopy. J. Phys. Chem. C 2016, 120 (17), 9393–9398. 10.1021/acs.jpcc.6b00180.

(72). Collier TA; Nash A; Birch HL; de Leeuw NH Intra-Molecular Lysine-Arginine Derived Advanced Glycation End-Product Cross-Linking in Type I Collagen: A Molecular Dynamics Simulation Study. Biophys. Chem 2016, 218, 42–46. 10.1016/j.bpc.2016.09.003. [PubMed: 27648753]

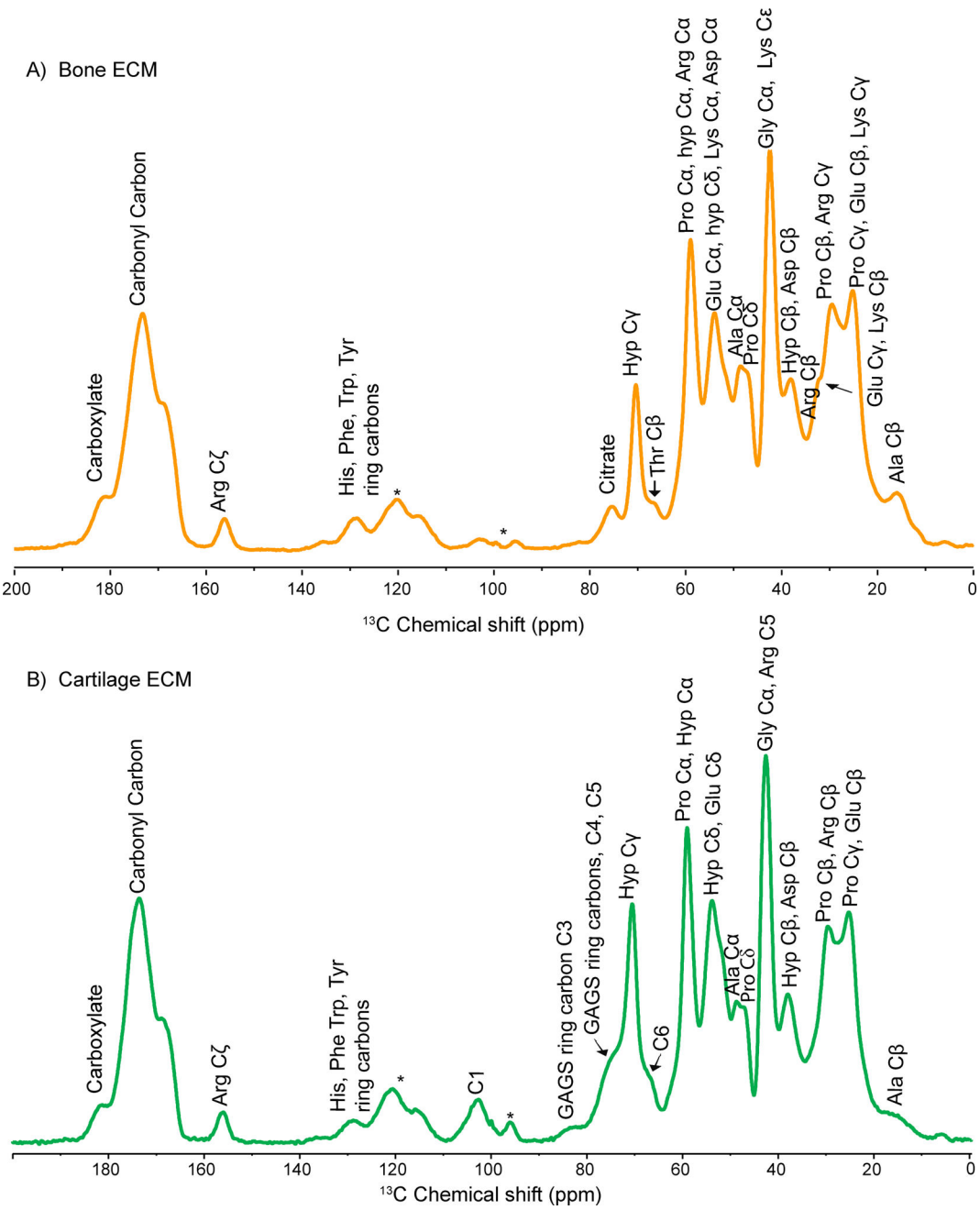

Figure 1:

Shows assigned resonances in natural abundance DNP enhanced 1D ^{1}H-^{13}C CPMAS spectra of A) bone ECM. And B) cartilage ECM.

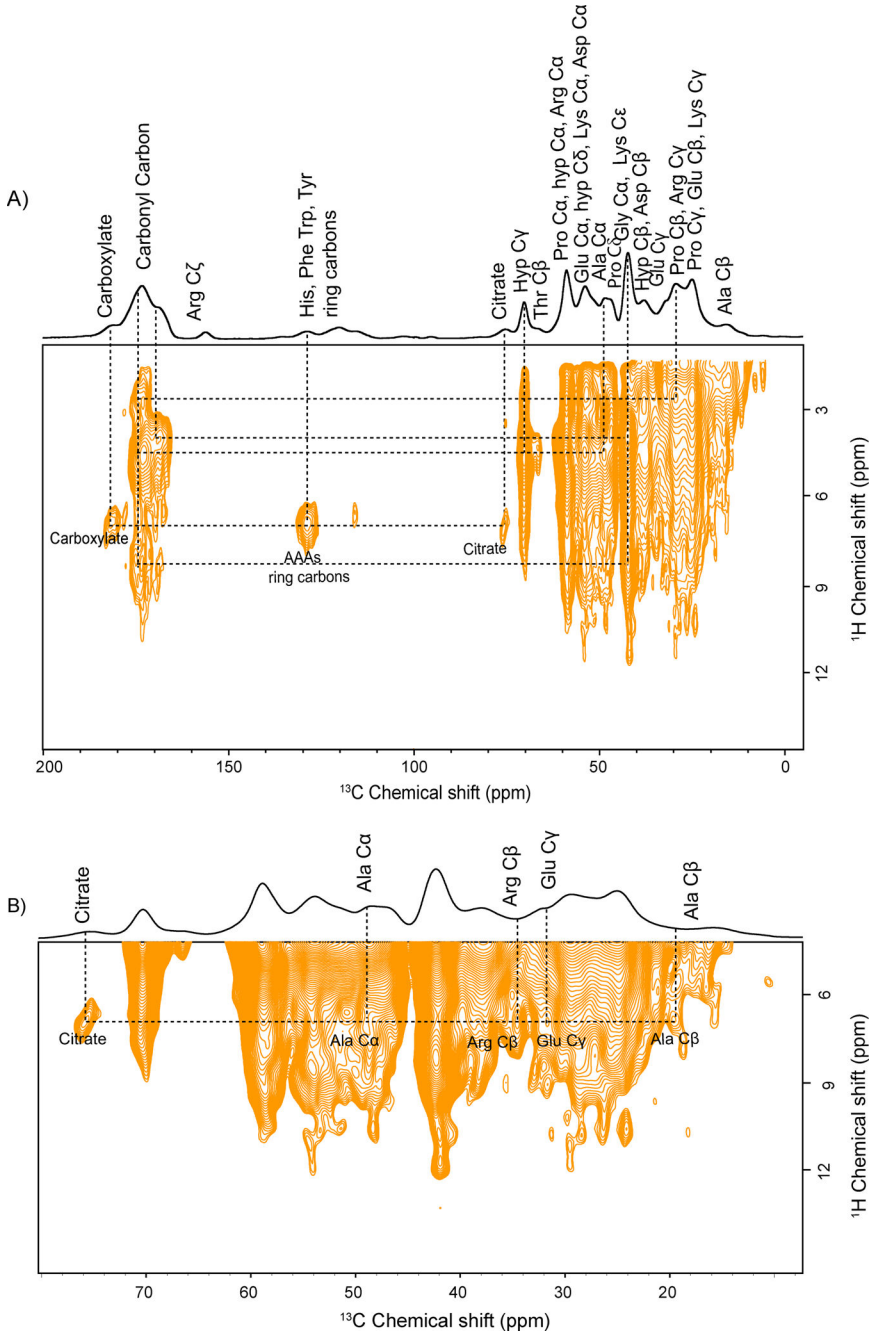

Figure 2:

A) Natural abundance 2D PMLG ^{1}H-^{13}C HETCOR spectrum of bone ECM and B) expanded region of fig.(A), showing molecular interaction between citrate and collagen residues along with other molecular interactions represented by the dotted line.

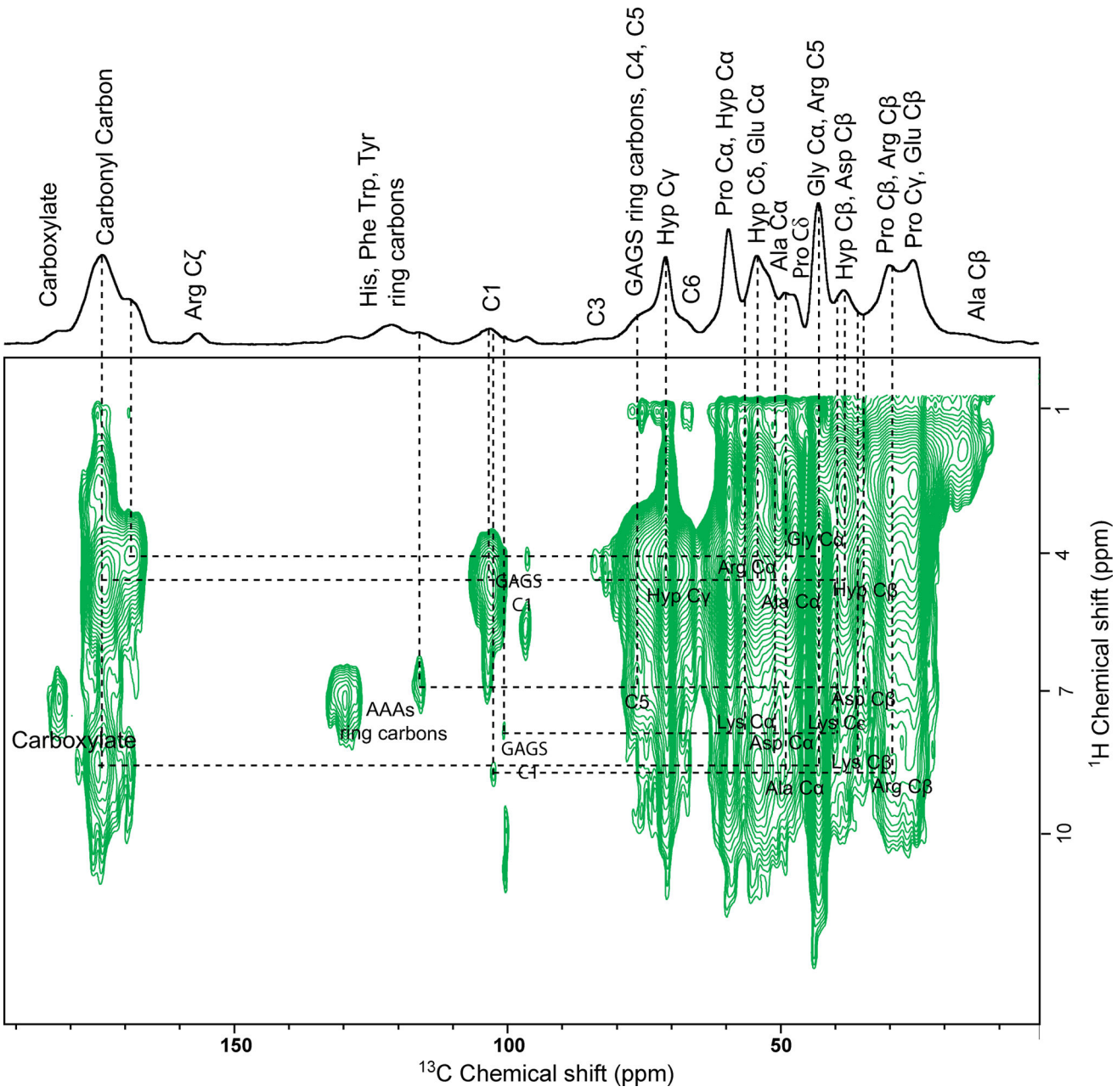

Figure 3:

Natural abundance 2D PMLG ^{1}H-^{13}C HETCOR spectrum of cartilage ECM shows molecular interaction between GAGS and collagen residues along with other molecular interactions represented by the dotted line.

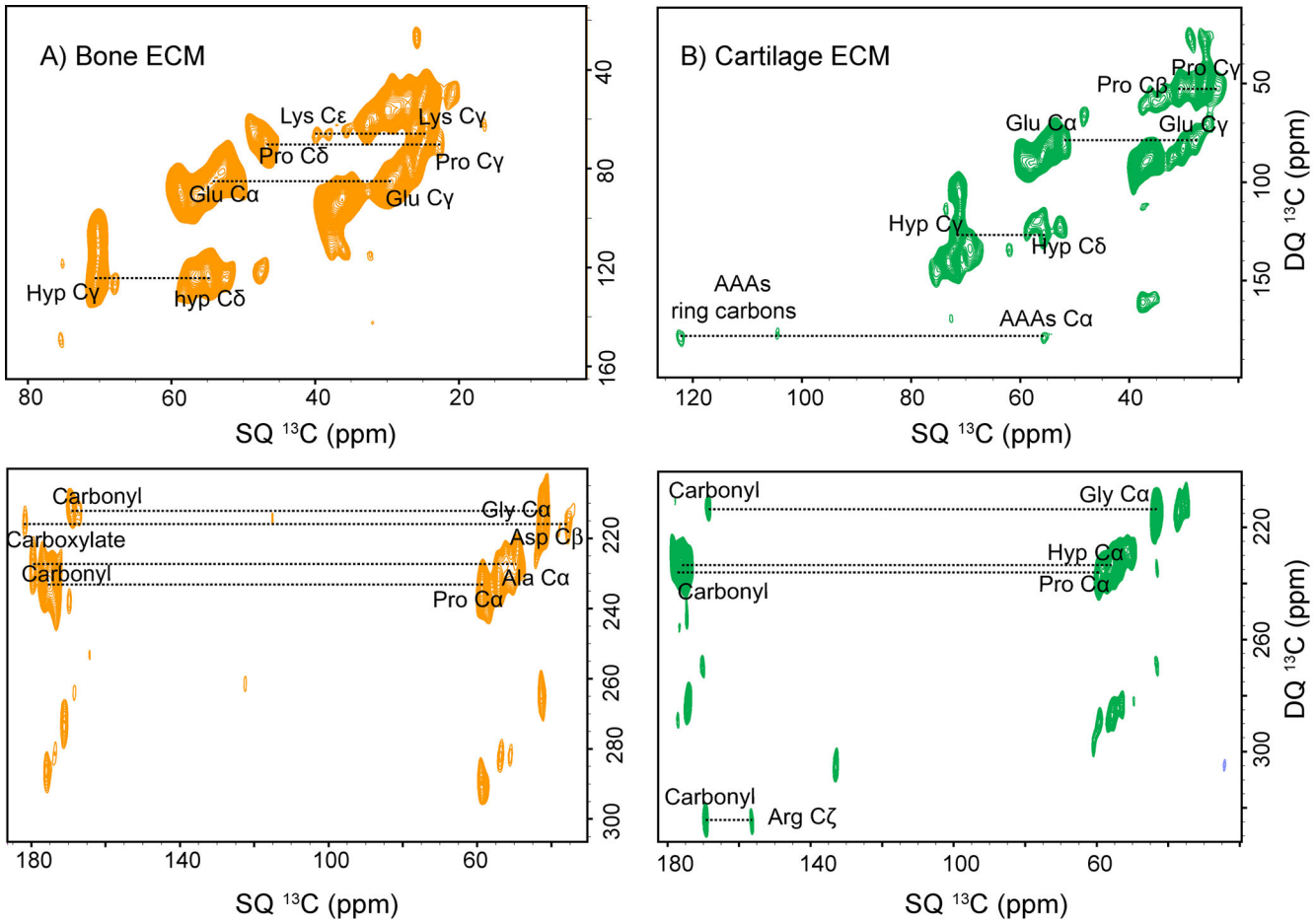

Figure 4:

Natural abundance 2D ^{13}C DQ-^{13}CQ spectra of A) bone ECM. B) cartilage ECM shows short-range (one bond) and long-range (more than one bond) correlation among ^{13}C resonances of collagen protein.

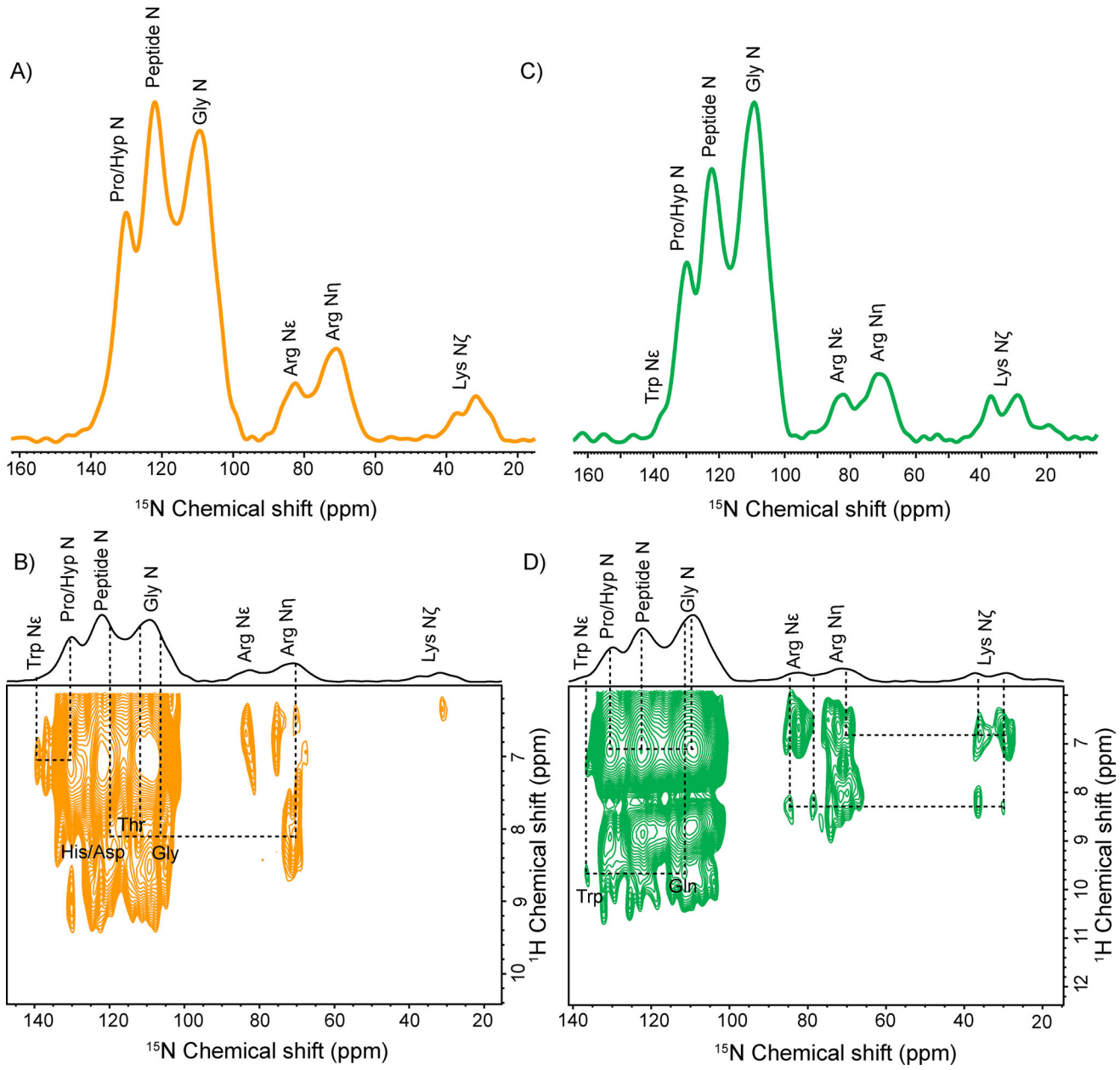

Figure 5:

Natural Abundance A) DNP enhanced 1D ^{1}H-^{15}N CPMAS of bone ECM with assigned resonances. B) 2D PMLG ^{1}H-^{15}N HETCOR spectrum of bone ECM with molecular interaction between ^{15}N resonances of various residues of collagen protein. C) DNP enhanced 1D ^{1}H-^{15}N CPMAS of Cartilage ECM with assigned resonances. B) 2D PMLG ^{1}H-^{15}N HETCOR spectrum of Cartilage ECM with molecular interaction between ^{15}N resonances of various residues of collagen protein.